Gap-state distribution in evaporated *a*-Si without and with posthydrogenation using space-charge-limited-current method

K. P. Chik and C. K. Yu
Department of Physics, The Chinese University of Hong Kong, Shatin, New Territory, Hong Kong

P. K. Lim
Department of Physics, Baptist College, Hong Kong

B. Y. Tong, P. K. John, and S. K. Wong*
Department of Physics, University of Western Ontario, London, Ontario, Canada N6A 3K7
(Received 22 May 1984)

The gap-state distribution of evaporated *a*-Si is studied by space-charge-limited-current method in the sandwich structure. A predominant peak in the gap-state distribution positioned at $E_c-0.52$ eV is found in annealed evaporated *a*-Si. This peak is supposed to arise from dangling bonds. After posthydrogenation, the gap-state density is found to be flat from below midgap up to $E_c-0.3$ eV, after which the gap-state density begins to rise exponentially towards E_c. Posthydrogenation has removed the gap states at $E_c-0.52$ eV.

I. INTRODUCTION

Although the amorphous state does not have a long-range order, it can still contain defects. Such defects may manifest themselves as traps in the mobility gap, thus influencing the electronic properties of an amorphous semiconductor. The important influence of defects in amorphous semiconductors has now been generally recognized. Many experiments involving both static and dynamic methods have been designed to probe the gap states. Spear and co-workers[1,2] studied glow-discharge (GD) *a*-Si-H samples and evaporated *a*-Si films using field-effect technique. For GD samples they reported that the gap-state distribution shows a minimum at midgap together with peaks lying at about 0.4 eV below conduction mobility edge E_c and at about 0.4 eV above valence mobility edge E_v. They suggested that the peaks may be identified with energy levels of a divacancy. In the case of the evaporated *a*-Si samples, they were only able to give a lower limit to the gap state density $g(E)$ of about 4×10^{20} $\mathrm{cm}^{-3}\mathrm{eV}^{-1}$. Later reports using different techniques, such as capacitance-voltage measurements,[3-5] deep-level transient spectroscopy (DLTS),[6] space-charge-limited-current (SCLC) method,[7,8] and other methods give conflicting results for GD *a*-Si-H samples. Field-effect experiments usually give a higher value for $g(E)$, which may be due to the influence of surface states. Some did not observe structure in the gap-state distribution. One should, however, bear in mind that the amorphous state is not a uniquely defined entity and different preparation conditions may lead to different defect structure. Hence diverse reports of $g(E)$ are not unexpected.

In this report, we do not anticipate solving the above conflict. A study on evaporated *a*-Si and on the effect of posthydrogenation using SCLC method is presented. Evaporated *a*-Si has the advantage that hydrogen is not incorporated at the outset into the amorphous matrix during the film formation. If the gap states are studied before and after hydrogenation, one can hope to gain some knowledge about defects that are present in pure amorphous silicon state and about the effect of hydrogen on such defects. The as-deposited evaporated *a*-Si has a very high density of gap states. SCLC experiments on such samples are not possible. By suitable annealing, the gap-state density can be reduced to a level where SCLC can be observed. The reduction of gap states by annealing may be attributed mainly to restructuring the more open network of the as-deposited state. We believe that the oxygen effect caused by the residual gas in 10^{-7}-Torr vacuum system is minor in comparison with the restructuring, so that the annealed state can still reflect the basic defect structure of the pure amorphous state. In the following, we report SCLC results on such annealed samples and on post-hydrogenated samples. With the assistance of some simple theoretical gap-state distribution models, concrete information about the gap states was obtained.

II. EXPERIMENTAL

Deposition of amorphous silicon films was performed by electron beam heating of pure-Si powder in a conventional vacuum coating system with a base pressure of approximately 10^{-7} Torr. The substrate was an electropolished stainless-steel sheet measuring 0.7×1.2 cm^2. The film thickness was 0.9 μm and the coating rate was 3 Å/s. A sandwich-type of metal/*a*-Si/stainless steel was used in all SCLC measurements. The deposited Si films on stainless steel substrate were then either subjected to postdeposition hydrogenation or suitably thermally annealed under dry nitrogen before the top electrodes were evaporated onto the upper Si surface. When the sandwich structure of the samples was completed, no further high-temperature treatment of the samples was performed. This precaution was undertaken to avoid any secondary effect of metal electrodes on the film structure.[9] Hydrogenation of the samples was done by means of a hydrogen

plasma source[10] and the posthydrogenated films will be designated by a-Si(H), while the unhydrogenated films will be designated as usual (a-Si). All SCLC measurements were carried out under high-vacuum ($<10^{-6}$ Torr) at temperatures between 200 and 500 K. Measurement temperatures were chosen in the range where hopping contribution to conduction is negligible. This was estimated from the temperature dependence of the temperature dependence of the dark dc conductivity at low voltage (Ohmic region).

Chromium, gold, and aluminum have been used as top electrode material. Usually all three kinds of metal dots (3 mm^2) could be deposited on the same sample so that the effect of top electrode metals on the SCLC measurements can be studied. Al was found to be unsatisfactory for SCLC measurement, while Au also presented some difficulties for hydrogenated samples. For these reasons we shall report results of a-Si samples with Cr or Au electrodes and results of a-Si(H) samples with Cr electrodes only.

III. THEORETICAL ASPECTS OF THE SCLC METHOD

A very comprehensive account of single-carrier injection in insulators containing simple trap distributions has been treated by Rose,[11] Lampert and Mark,[12] Lampert and Schilling,[13] Van der Ziel,[14] and Kao and Hwang.[15] In the following discussions, single-electron injection is presumed throughout, and the free electrons are considered to be injected into the conduction band above the mobility edge E_c. Since both unhydrogenated and hydrogenated Si films are of n type, the above presumption is justified. To ensure conduction above the mobility edge, injection experiments should therefore be done at temperatures where hopping conduction contribution becomes negligible. It is further assumed that the mobility of the free carriers is independent of electric field and is only slightly affected by the presence of traps.

At low field, the thermally generated carrier density is predominant and the conduction is ohmic. The current density J is given by Ohm's law,

$$J_0=qn_0\mu V_0/L \ , \tag{1}$$

and

$$n_0=N_c\exp[-(E_c-E_{F0})/kT] \ , \tag{2}$$

where μ is the drift mobility, q the electronic charge, V_0 the applied voltage, L the sample thickness, N_c the effective density of states at the conduction band, and E_{F0} the thermal equilibrium Fermi level.

The following cases of SCLC are of special interest.

(a) *Discrete shallow traps at energy E_t.*[12] When the sample contains traps, a large fraction of the injected space charge condenses into these traps. The ratio θ of free to trapped electrons is then

$$\theta=\frac{N_c}{gN_t}e^{-(E_c-E_t)/kT} \ . \tag{3}$$

where N_t is the density of electron traps at E_t and g the degeneracy factor of the traps. For convenience we take $g=1$ hereafter. The current J is now given by[12]

$$J=(9/8)\epsilon\epsilon_0\theta\mu V^2/L^3 \ , \tag{4}$$

where ϵ is the dielectric constant of Si and ϵ_0 is the permittivity constant. The J-V characteristics of such samples should begin with an Ohmic region crossing over to a V^2 dependence. The slope γ of the $\log J$-$\log V$ curve is then 2. The crossover voltage V_x is

$$V_x\approx(qL^2/\epsilon\epsilon_0)N_t\exp[-(E_t-E_{F0})/kT] \ . \tag{5}$$

According to Eq. (5) V_x should increase as temperature is raised. The temperature dependence of V_x will yield information about E_t and N_t.

(b) *Discrete deep traps at E_t.*[12] The traps are considered deep when E_t lies below E_{F0}. In thermal equilibrium, the density of unfilled electron traps is

$$p_{t0}\approx N_t\exp[-(E_{F0}-E_t)/kT] \ . \tag{6}$$

These traps will be filled up when the applied voltage is increased. Any subsequently injected electrons are then free to move in the sample and the current flow increases rapidly with further voltage increase. Thus conduction has crossed over from Ohmic to the case of trap-filled-limit conduction. The crossover voltage V_x is given by [analogous to Eq. (5)]

$$V_x\approx qp_{t0}L^2/\epsilon\epsilon_0 \ . \tag{7}$$

Hence the value of V_x depends on the position of the deep trap relative to E_{F0}.

(c) *Gaussian distribution of traps.*[15,16] Suppose the trap distribution is Gaussian,

$$g(E)=\frac{N_t}{(2\pi)^{1/2}\sigma_t}e^{-(E-E_{tm})^2/2\sigma_t^2} \ , \tag{8}$$

where E_{tm} is the electron trapping energy level with a maximum trap density and σ_t the standard deviation of the Gaussian function. Then for shallow traps, we still have a V^2 law given by Eq. (4) with θ now being modified as

$$\theta=\frac{N_c}{N_t}e^{-(E_c-E_{tm})/kT+(1/2)(\sigma_t/kT)^2} \ , \tag{9}$$

and the crossover voltage becomes

$$V_x\approx\frac{qL^2}{\epsilon\epsilon_0}N_t\exp\{-[E_{tm}-E_{F0}+\tfrac{1}{2}(\sigma_t^2/kT)]/kT\} \ . \tag{10}$$

For deep traps, $E_{tm}<E_{F0}$, the current density J is

$$J\propto V^{m+1} \ , \tag{11}$$

$$V_x\propto\exp\{[(E_{F0}-E_{tm})/kT]^{1/m}\} \ , \tag{12}$$

and

$$m=[1+2\pi\sigma_t^2/(16k^2T^2)]^{1/2} \ . \tag{13}$$

(d) *Traps distributed uniformly within the energy gap.*[11,15,17] Suppose the traps are distributed uniformly from energy E_l to E_u ($E_u>E_l$) with a density per unit energy interval of g_t'. Then according to Kao and Hwang,[15] the current density is given by

$$J=2q\epsilon\epsilon_0 N_c \frac{V}{L} e^{(E_l-E_u)/kT} e^{(2\epsilon\epsilon_0 V/qg_t' kTL^2)} , \quad (14)$$

and the crossover voltage from Ohmic to SCLC becomes almost temperature independent, namely

$$V_x=\frac{qg_t' kTL^2}{2\epsilon\epsilon_0}[\ln(n_0/2N_c)+(E_u-E_l)/kT]$$
$$=\frac{qg_t' L^2}{2\epsilon\epsilon_0}[E_u-E_l-(E_c-E_{F0})-0.693kT] . \quad (15)$$

(e) *Calculation of $g(E)$ directly from J-V curves.* From the above discussions, it is obvious that the trap distribution $g(E)$ can be obtained directly from the J-V characteristics. This method has been described by Nespurek and Sworakowski[18] and den Boer.[19] In our analysis of results, we follow closely the method developed by these authors.

Suppose in thermal equilibrium, the concentration of filled electron traps is n_{t0}. When a voltage V is applied, the free carrier density becomes

$$n=N_c\exp[-(E_c-E_{Fn})/kT] \quad (16)$$

and

$$J=nq\mu V/L , \quad (17)$$

where E_{Fn} is the quasi-Fermi-level. The concentration of filled traps is now n_t. Assuming a continuous-trap distribution function $g(E)$,

$$n_t-n_{t0}\approx \int_{E_{F0}}^{E_{Fn}} g(E)dE , \quad (18)$$

or

$$dn_t=g(E)dE_{Fn} . \quad (19)$$

The injected charge per unit area Q can be expressed approximately as

$$Q=K\epsilon\epsilon_0 V/L . \quad (20)$$

K is a factor lying between 1 and 2 accounting for the nonuniformity of the internal field. If most of the injected charge is trapped, then

$$qL(n_t-n_{t0})=K\epsilon\epsilon_0 V/L , \quad (21)$$

or

$$dn_t=(K\epsilon\epsilon_0/qL^2)dV . \quad (22)$$

Differentiating Eq. (17) with respect to $\ln V$, one gets

$$\frac{d(\ln J)}{d(\ln V)}-1=\frac{d(E_{Fn}/kT)}{(1/V)dV} . \quad (23)$$

Writing $\gamma=d(\ln J)/d(\ln V)$ and using Eqs. (19) and (22), one finally obtains

$$g(E)=\frac{K\epsilon\epsilon_0 V}{qL^2 kT(\gamma-1)} . \quad (24)$$

Equation (24) is the fundamental equation used for the evaluation of experimental data to get $g(E)$ directly from a log-log plot of the J-V curve and is true as long as μ is independent of applied field. In SCLC experiments, one is measuring the steady state current. The effect of traps on electron conduction is reflected in Eq. (16). Thus one can expect that the mobility μ in Eq. (17) behaves in the same way as μ in Eq. (1). Hence the relative shift ΔE_F of the quasi-Fermi-level with respect to E_{F0} for a given voltage V is easily evaluated by taking the ratio of Eq. (17) and Eq. (1), namely,

$$\Delta E_F=E_{Fn}-E_{F0}=kT[\ln(J/J_0)-\ln(V/V_0)] . \quad (25)$$

For the evaluation of $g(E)$ from Eq. (24), one requires the slope as a function of V along a $\log J$-$\log V$ curve. If the experimental points along the $\log J$-$\log V$ curve are sufficiently close and the J-V curve is slowly varying locally, one can approximate each small section of the curve as a straight line and find the slope γ by using linear least-squares fit to three, four, or five neighboring data points. Out of the three values of γ, the one with the least deviation is taken as the true γ for a given V. This procedure is repeated for each data point, using a computer. By means of this method of local linear-least-squares fit (LSF), one can smooth out fluctuations due to experimental errors. We have compared this method with the step-by-step method of den Boer,[19] and found that the two methods give essentially the same result except that the local fit method produces a smoother curve. All our results were analyzed by the LSF method. The constants used in our analysis are $K=1.5$ and $\epsilon=11.7$ for silicon.

IV. EXPERIMENTAL RESULTS AND ANALYSIS

A. a-Si: J-V curves and gap state distribution

As-deposited unhydrogenated a-Si samples have a very high density of gap states so that hopping conduction is predominant well above room temperature. Current injection in such samples even at high temperatures is difficult. By suitable annealing hopping conduction can be substantially reduced[20] so that current injection can be effected easily at or above room temperature. Figure 1 shows

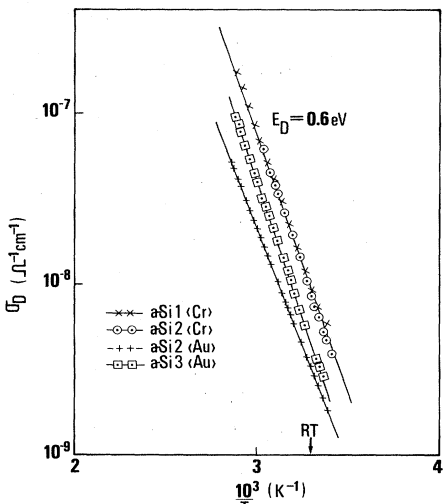

FIG. 1. Temperature dependence of dark electrical conductivity σ_D of a-Si samples annealed at 678 K using Cr or Au upper electrodes.

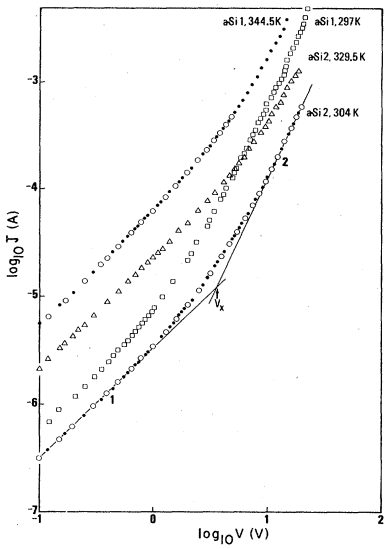

FIG. 2. J-V curves for a-Si1 and a-Si2 (unhydrogenated). Solid dots represent data prints obtained under reverse bias.

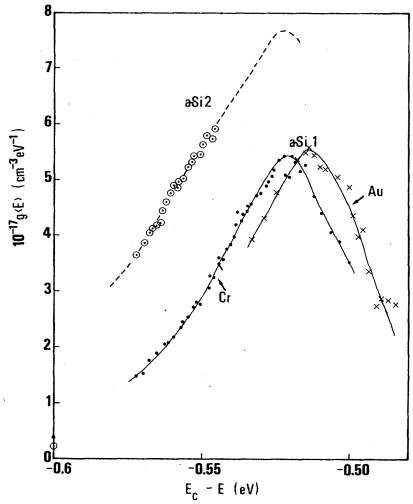

FIG. 3. Density of gap-state distribution $g(E)$ for a-Si1 and a-Si2. Position of Fermi level at -0.6 eV is indicated by ⊕.

that the Arrhenius plots for the dark electrical conductivity σ_D for three samples annealed at 678 K using Cr or Au upper electrodes. It can be seen that the Arrhenius plots are linear to down below room temperature. All our results on a-Si refer to samples annealed around this temperature. Both Cr and Au electrode samples give similar results with an average $E_D=0.6$ eV and with the preexponential factor σ_0 between 10 and 500 $\Omega^{-1}\,\mathrm{cm}^{-1}$ where $\sigma_D=\sigma_0\exp(-E_D/kT)$. These values are very close to the values obtained on a similar sample measured in planar configuration, namely $E_D=0.68$ eV and $\sigma_0=300$ $\Omega^{-1}\,\mathrm{cm}^{-1}$.[21] We may assign 0.6 eV below E_C as the position of E_{F0} in our a-Si samples.

Figure 2 shows the log$J$-log$V$ plots for typical samples a-Si1 and a-Si2. Also shown are the J-V curves in reversed bias (indicated by small solid dots). The curves in opposite bias are exactly identical. In general, all curves show a gradual transition from Ohmic conduction at low field to an approximate V^2 law conduction. The crossover voltage V_x for different samples are listed in Table I. The best J-V curves are obtained at temperatures between 290 and 330 K. At higher temperatures, the Ohmic region extends to a much higher electric field so that only a small range of current injection can be investigated. As a result, the determination of V_x becomes less accurate.

The density of gap-state distribution $g(E)$ deduced from several J-V curves of a-Si prepared under the same condition is shown in Fig. 3, using an average value of $E_{F0}=0.6$ eV. The range of E that can be swept through is only about 0.15 eV above E_{F0}. However, one can see clearly that there is a peak in the gap distribution centered at about 0.08 eV above E_{F0} (i.e., $E_c-E_t\approx 0.52$ eV) with a $g(E)$ peak value of about 6×10^{17} $\mathrm{cm}^{-3}\,\mathrm{eV}^{-1}$ for a-Si1. The curve for a-Si2 suggests that this sample has a slightly higher gap-state density with an estimated peak of $\sim 8\times10^{17}$ $\mathrm{cm}^{-3}\,\mathrm{eV}^{-1}$. The Fermi-level position deduced from Arrhenius plot of σ_D, such as shown in Fig. 1, can have an error of ±0.05 eV, which is of the order of the range of E that can be swept through in the injection experiment. Fortunately, the evaluation of $g(E)$ depends on ΔE_F rather than on the absolute value of E_{F0}. Our results show definitely a gap-state level lying above the Fermi level.

There is another way to check the relative positions of the gap state distribution deduced from different J-V curves. Since the samples are prepared under the same condition, one can assume that N_c and μ are the same. At high-injection level, the current flowing through the sample should be less affected by electrode effects. Using

TABLE I. Comparison between experimental and theoretical crossover voltage for current injection in evaporated a-Si. Values in parentheses represent the ratio $V_x(T_2)/V_x(T_1)$.

Sample	Temperature (K)	V_x^{expt} (V)		Discrete trap model V_x^{cal} (V)		Gaussian trap model V_x^{cal} (V)		N_t^{cal} (cm^{-3})
a-Si1Cr	$T_1=297$	1.7	(2.3)	3.2	(1.5)	1.5	(1.7)	4.5×10^{16}
	$T_2=344.5$	3.9		4.95		2.6		
a-Si1Au	$T_1=305$	1.7	(1.5)	3.5	(1.2)	1.7	(1.2)	
	$T_2=324$	2.5		4.2		2.1		
a-Si2Cr	$T_1=304$	3.5	(1.5)	4.7	(1.2)	1.3	(1.6)	10^{17}
	$T_2=329.5$	5.2		5.8		2.1		
a-Si2Au	310	5.7		4.9		1.5		

suffix 1 and 2 to denote two different samples, we can write

$$J_1 = N_c q\mu \frac{V_1}{L} \exp[-(E_c - E_{Fn1})/kT] , \quad (26)$$

$$J_2 = N_c q\mu \frac{V_2}{L} \exp[-(E_c - E_{Fn2})/kT] . \quad (27)$$

Hence the relative position of the quasi-Fermi-levels of the two samples at the given J-V values is

$$\Delta E_{Fn} = E_{Fn2} - E_{Fn1} = kT \ln \frac{J_2}{J_1} \frac{V_1}{V_2} . \quad (28)$$

In this way we have checked the relative positions of the deduced $g(E)$ and found that the results are consistent with a Fermi level $E_{F0} \approx 0.6$ eV. In our preliminary report,[22] we have shown one sample with a gold electrode which gives $E_D = 0.8$ eV and $\sigma_0 = 4 \times 10^5$ $\Omega^{-1}\text{cm}^{-1}$. Taking this value as true E_{F0} would give a second peak of $g(E)$ at $E = 0.7$ eV below E_c. To test this, Eq. (28) is used to locate this peak relative to the peak at 0.52 eV. Calculations showed that the two peaks should coincide. The corrected position is shown in Fig. 3 by the curve with crosses. This analysis shows that the experimental value of $E_D = 0.8$ eV is not the true E_{F0} as originally proposed in Ref. 22. This discrepancy may be due to electrode effects.

The gap-state distribution in Fig. 3 suggests that the a-Si samples may be described by a model with shallow traps. This is consistent with the approximate V^2 behavior of the J-V curve in Fig. 2. Then we can apply the theory discussed in Sec. III to analyze our results. Assuming the traps to spread out in an energy range of about 0.1 eV, the trap density N_t in our samples is about 6×10^{16} cm^{-3} for a-Si1 and 8×10^{16} cm^{-3} for a-Si2. Taking $E_t - E_{F0} = 0.08$ eV, the crossover voltage V_x is calculated from Eq. (5). The results are shown in Table I. It can be seen V_x^{cal} agrees reasonably well with the experimental values, though V_x^{cal} gives a weaker temperature dependence. The analysis is repeated using a model of Gaussian trap distribution using Eqs. (8)—(10), and the results are also listed in Table I. In this case, we take $\sigma_t = 0.025$ eV and $N_t(E)^{\max} = 6 \times 10^{17}$ $\text{cm}^{-3}\text{eV}^{-1}$ for a-Si1 and $\sigma_t = 0.045$ eV and $N_t(E)^{\max} = 8 \times 10^{17}$ $\text{cm}^{-3}\text{eV}^{-1}$ for a-Si2. From Eq. (8) we get $N_t = 4.5 \times 10^{16}$ cm^{-3} and 10^{17} cm^{-3} for the two samples, respectively. In this case, the Gaussian model gives a better agreement in the temperature dependence of V_x. In view of the approximations used in the theory and the arbitrary chosen value for K, we should not overly stress the absolute values of V_x; however, we can consider the agreement as a solid support for the presence of a trap level above the Fermi level.

B. a-Si(H) samples

After hydrogenation, a-Si(H) gives a straight-line Arrhenius plot of σ_D down to below room temperature. Hence current-injection experiments can be carried out from room temperature upward. The activation energy E_D is found to lie between 0.43 and 0.47 eV. All a-Si samples after hydrogenation show a Fermi-level shift toward the conduction-band edge. This shift was recorded in measurements with both sandwich and planar configurations. One possible explanation is that before hydrogenation the Fermi level is pinned by defects at near 0.6 eV, and after hydrogenation it is freed to move to its equilibrium position. The shift direction may indicate that there is an asymmetry in the tail-state distributions near the conduction and the valence band. Theoretical calculations have shown[23] that after hydrogenation, the antibonding states crowd near the bottom of the conduc-

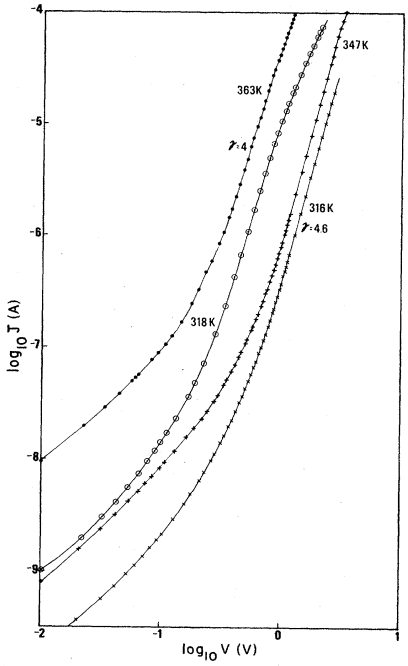

FIG. 4. J-V curves of a-Si(H): —●—●—●— and —⊙—⊙—⊙— represent a-Si(H)1 and —+—+—+— and —×—×—×— represent a-Si(H)2.

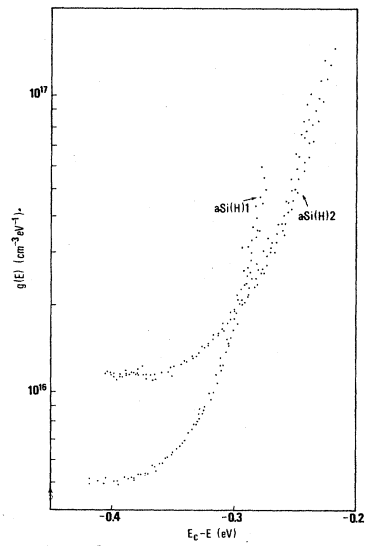

FIG. 5. Density of gap-state distribution $g(E)$ for a-Si(H)1 and a-Si(H)2. Each curve represents data obtained from several J-V curves measured at different temperatures.

tion band while the bonding states merge deep into the valence band.

The typical $\log J$-$\log V$ curves for a-Si(H)1 (—⊙—⊙—⊙—) and a-Si(H)2 (—×—×—×—) which have been hydrogenated separately at different temperatures are shown in Fig. 4. The general features of these curves are different from those of the a-Si samples. After an initial Ohmic region, the J-V curve rises rapidly with increasing voltage, leading to $\gamma \approx 4$ which is almost temperature independent. Furthermore, the crossover voltage V_x is also almost temperature independent. Analyses of the J-V curves using LSF method, give the trap distribution as shown in Fig. 5, taking $E_c - E_{F0} = -0.45$ eV for both samples. The curves in Fig. 5 show that $g(E)$ decreases exponentially from $E = 0.2$ eV below E_c and tends to level off around $E \approx 0.4$ eV with a value of 5×10^{15} cm^{-3}eV^{-1} for a-Si(H)1 and 10^{16} cm^{-3}eV^{-1} for a-Si(H)2. Although $g(E)$ for E beyond $E = 0.45$ eV cannot be measured directly in the present experiments, the observed curves still suggest that the gap states at 0.52 eV found in a-Si samples are removed by hydrogenation. This conclusion is well supported by a careful analysis of J-V curves, as shown in the following.

If there *were* a peak at 0.52 eV, the J-V curves would be explained by a model of deep traps. Suppose we have a Gaussian distribution of traps at 0.07 eV below E_{F0}. Taking a-Si(H)1 as an example, $\gamma = 4$ or $m = 3$ at 317 K. According to Eq. (13), σ_t is found to be 0.12 eV. Since J is proportional to V^{m+1}, one can estimate the temperature dependence of γ. Taking $\sigma_t = 0.12$ eV, $\gamma(317\text{ K}) = 4$. Similar consideration at 360 K gives $\gamma(360\text{ K}) = 3.6$. Experimentally γ is practically unchanged. On the contrary, both the voltage and temperature dependence of J can be well described by a model for traps distributed uniformly within the mobility gap [Sec. III, part (d)]. At low voltage in the Ohmic region,

$$J_0 = q\mu n_0 (V/L) .$$

Hence,

$$\ln J_0 = \ln V + C_1(T) . \tag{29}$$

From Eq. (14) we have

$$\ln J = \ln V + C_2(T) + (2\epsilon\epsilon_0 / qg'kTL^2)V . \tag{30}$$

Subtracting Eq. (30) from Eq. (29), we obtain

$$\Delta \ln J = \ln J - \ln J_0 = SV + C(T) , \tag{31}$$

where

$$S = \frac{2\epsilon\epsilon_0}{qg'kTL^2} . \tag{32}$$

$C_1(T)$, $C_2(T)$, and $C(T)$ are functions of temperature but not of V. Thus plotting $\Delta \ln J$ (found on a single J-V curve) against V should give a straight line with slope S given by Eq. (32). The linearity of the $\Delta \log J$-versus-V plots is demonstrated in Fig. 6 for both a-Si(H)1 and a-Si(H)2. Figure 7 shows the inverse temperature dependence of S. From the experimental value of S, g' the density of trap states per unit energy interval can be evaluated. Using $S(318\text{ K}) = 8.7$ per volt for a-Si(H)1 and $S(316\text{ K}) = 3.8$ per volt for a-Si(H)2, one gets a trap density per eV of 7×10^{15}cm^{-3}eV^{-1} and 1.6×10^{16} cm^{-3}eV^{-1} for

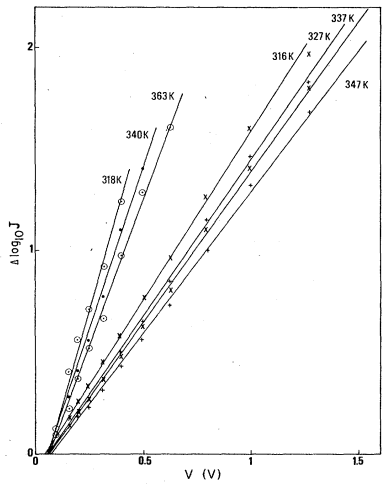

FIG. 6. $\Delta \log J$-vs-V plots for a-Si(H)1 and a-Si(H)2 obtained from J-V curves at different temperatures. The curves at 318, 340, and 363 K correspond to a-Si(H)1 and the rest correspond to a-Si(H)2.

the two samples, respectively. These values agree excellently with that deduced from the LSF method. Using Eq. (15), one can further estimate the range of E where $g(E)$ is expected to be constant. Taking $V_x = 0.1$ V, one gets $E_u - E_l \approx 0.5$ eV and V_x changes by less than 20% when temperature differs by 100 K. This explains the weak temperature dependence of V_x found experimentally. If we take $E_u = 0.4$ eV from Fig. 5, then $E_l = 0.9$ eV. This means that the gap-state density $g(E)$ is flat below midgap.

On the other hand, $g(E)$ starts to rise smoothly at about $E_c - 0.3$ eV toward E_c, suggesting an exponential band tail. By extrapolating the $g(E)$ curves in Fig. 5 to $E_c - E = 0$, one obtains $g(E_c) \approx 10^{22}$ and 2×10^{20} cm^{-3}eV^{-1} for a-Si(H)1 and a-Si(H)2, respectively. These values are comparable to the value suggested by Spear and LeComber[1] who found $g(E_c) \approx 4 \times 10^{20}$ cm^{-3}eV^{-1} for GD a-Si(H) samples.

V. DISCUSSION

In this paper, we are able to demonstrate that SCLC experiments can be successfully applied to amorphous semi-

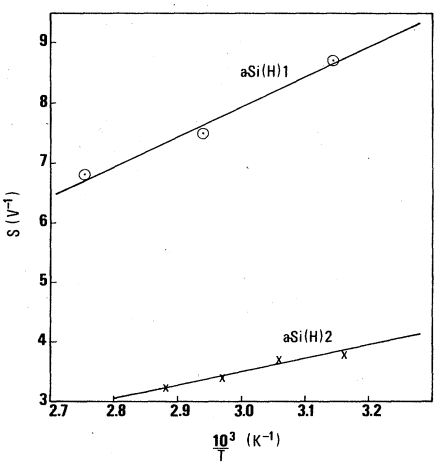

FIG. 7. Temperature dependence of S (see text).

conductors to obtain information about gap states. The gap-state density obtained by this method is less affected by surface state since the injected current passing through the sample depends on the bulk property. Evaporated a-Si usually has a high density of gap states. As reported by Madan *et al.*,[24] evaporated samples showed very small field effects. Similarly, SCLC cannot be observed in samples with high trap density. Hence we studied evaporated a-Si in the annealed state. Annealing is able to release much of the strains in the as-deposited state, giving films with simpler defects. For example, the EPR signal (g value$=2.005$) of our as-deposited a-Si is broad and asymmetric. After annealing above 600 K, the EPR signal becomes sharp and symmetric with a typical linewidth of about 6 G. At the same time, such samples show appreciable SCLC at reasonable electric fields indicating that the gap-state density is indeed reduced.

The gap-state distribution of evaporated a-Si (without hydrogen) is obtained for the first time by SCLC method. The distribution shows a large peak at 0.52 eV below E_c (see Fig. 3). One may note, that this distribution cannot be compared directly with data which are obtained from GD a-Si, which contains a hydrogen modifier. There have been suggestions that a divacancy may give rise to the two energy levels at $E_c-0.4$ eV and $E_c-1.2$ eV found in GD a-Si(H) samples because these levels are very similar to the V_2^- and V_2^+ levels in crystalline Si. As Davis[25] has warned, the divacancy model may be overly simple and the divacancy in a-Si may not necessarily give rise to the same energy levels in the gap as in crystalline silicon. Our result for evaporated a-Si does not fit into the divacancy defect model.[26] The Fermi level of our a-Si samples lies around $E_c-0.6$ eV, which is below the level at $E_c-0.52$ eV. Thus without current injection, divacancies, if present in the samples, would be neutral. Neutral divacancies are nonparamagnetic and should not be detected by EPR, in contrary to experimental observations. Recently, Okushi *et al.*[27] reported a level at $E_c-0.5$ eV in n-doped a-Si(H), which they attributed to doubly occupied dangling-bond level. This level is close to the level we observed.

The SCLC method has its limitation. The range of E_F that can be swept through in the experiments is quite small, about 0.2 eV. In addition, only gap states above the Fermi level can be studied. This limitation is more conspicuous in the experiments on a-Si(H) samples. Here $g(E)$ is almost flat above E_F before it rises steeply towards E_c. The interesting range of $g(E)$ would therefore lie below E_F. However, some hidden information can be recovered by analyzing the experimental results carefully in combination with theoretical gap state models. In this way, we are able to show that $g(E)$ in our a-Si(H) samples is flat down to below midgap. The overall picture of a-Si(H) samples is a structureless $g(E)$ distribution with an exponential band tail toward E_c. This is in sharp contrast to the $g(E)$ of GD a-SI(H) of Ref. 2, which shows structure and a minimum. There has been recently controversy about the interpretation of the field-effect data which can lead to either a $g(E)$ with or without structure.[28,29] Other experiments[3] also report an exponential $g(E)$ decay similar to our observations. It is possible that the fine details of $g(E)$ much depend on the preparation conditions of the samples. Due to the discrepancies of results among different reports, we cannot conclude whether there are substantial difference in gap state distributions between a-Si(H) prepared by post-evaporation hydrogenation and the GD a-Si(H) films.

VI. CONCLUSION

In this paper, we have shown that SCLC method has been successfully applied to study the gap-state distribution in evaporated a-Si in the annealed state and in the posthydrogenated state. Without hydrogenation, the gap-state distribution exhibits a peak at $E_c-0.52$ eV, which may be attributed to dangling bonds. After posthydrogenation, this peak is removed producing a flat $g(E)$ distribution extending from down below Fermi level up to about $E_c-0.3$ eV. From that energy onward, $g(E)$ rises exponentially toward E_c. It seems that $g(E)$ in the posthydrogenated a-Si(H) samples shows no structure and no minimum.

*Department of Chemistry, University of Western Ontario, London, Ontario, Canada N6A 3K7.

[1]W. E. Spear and P. G. LeComber, J. Non-Cryst. Solids **8—10**, 727 (1972).

[2]P. G. LeComber, A. Madan, and W. E. Spear, J. Non-Cryst. Solids **11**, 219 (1972).

[3]G. M. Döhler and M. Hirose, in *Proceedings of the Seventh International Conference on Amorphous and Liquid Semiconductors,* edited by W. E. Spear (Edinburgh University, Edinburgh, 1977), p. 372.

[4]N. B. Goodman and H. Fritzsche, Philos. Mag. B **42**, 149 (1980).

[5]P. Viktorovitch and D. Jousse, J. Non-Cryst. Solids **35/36**, 569 (1980).

[6]J. D. Cohen, C. V. Lang, and J. P. Harbison, Phys. Rev. Lett. **45**, 197 (1980).

[7]S. Ashok, A. Lester, and S. J. Fonash, IEEE Trans. Electron Devices Lett. **EDL-1**, 200 (1980).

[8]K. D. Mackenzie, P. G. LeComber, and W. E. Spear, Philos. Mag. **46**, 377 (1982).

[9]S. R. Herd, P. Chandhari, and M. H. Brodsky, J. Non-Cryst. Solids **7**, 309 (1972).

[10]B. Y. Tong, P. K. John, S. K. Wong, and K. P. Chik, Appl. Phys. Lett. **38**, 789 (1981).

[11]A. Rose, Phys. Rev. **97**, 1538 (1955).

[12]M. A. Lampert and P. Mark, *Current Injection in Solids* (Academic, New York, 1970).

[13]M. A. Lampert and R. B. Schilling, *Semiconductors and Semimetals* (Academic, New York, 1970), Vol. 6, p. 1.

[14]A. Van der Ziel, *Semiconductors and Semimetals* (Academic, New York, 1979), Vol. 14, p. 195.

[15]K. C. Kao and K. Hwang, *Electrical Transport in Solids* (Pergamon, New York, 1981).

[16]J. S. Bonham, Aust. J. Chem. **26**, 927 (1973).

[17]R. S. Muller, Solid-State Electron. **6**, 25 (1963).

[18]S. Nespurek and J. Sworakowski, J. Appl. Phys. **51**, 2098

(1980).
[19]W. den Boer, J. Phys. (Paris) Colloq. **42**, C4-451 (1981).
[20]K. P. Chik, S. Y. Feng, and S. K. Poon, Solid State Commun. **33**, 1019 (1980).
[21]K. C. Koon, M. Philos. thesis, The Chinese University of Hong Kong, 1983 (unpublished).
[22]K. P. Chik, C. K. Yu, P. K. Lim, B. Y. Tong, S. K. Wong, and P. K. John, J. Non-Cryst. Solids **59/60**, 285 (1983).
[23]F. C. Choo and B. Y. Tong, Solid State Commun. **25**, 385 (1978).
[24]A. Madan, P. G. LeComber, and W. E. Spear, J. Non-Cryst. Solids **20**, 239 (1976).
[25]E. A. Davis, in *Amorphous Semiconductors,* edited by M. H. Brodsky (Springer, Berlin, 1979), p. 41.
[26]A. Seeger and K. P. Chik, Phys. Status Solidi **29**, 455 (1968).
[27]H. Okushi, T. Takahama, Y. Tokumaru, S. Yamasaki, H. Oheda, and K. Tanaka, Phys. Rev. B **27**, 5184 (1983).
[28]N. B. Goodman and H. Fritzsche, Philos. Mag. B **42**, 149 (1980).
[29]M. J. Powell, Philos. Mag. B **43**, 93 (1981).